

A prototype station of the IceCube-Gen2 Surface Array at the Pierre Auger Observatory

Stef Verpoest,^{a,*} Carmen Merx^b and Benjamin Flaggs^a on behalf of the IceCube-Gen2¹ and Pierre Auger^{c,2} Collaborations

(a complete list of authors can be found at the end of the proceedings)

^a*Bartol Research Institute, Department of Physics and Astronomy, University of Delaware*

^b*Institute for Astroparticle Physics (IAP), Karlsruhe Institute of Technology (KIT),
76021 Karlsruhe, Germany*

^c*Observatorio Pierre Auger, Av. San Martín Norte 304, 5613 Malargüe, Argentina
E-mail: verpoest@udel.edu, analysis@icecube.wisc.edu,
spokespersons@auger.org*

The detection of extensive air showers using radio antennas has evolved into a mature technique, complementing particle detector arrays by providing sensitivity to the longitudinal development of the showers and enabling an independent determination of the cosmic-ray energy. Both the Pierre Auger Observatory in Argentina and the IceCube Neutrino Observatory at the South Pole have been undergoing upgrades, including the integration of radio antennas. The next-generation neutrino detector IceCube-Gen2 will also feature a surface array for PeV-EeV cosmic-ray detection, consisting of scintillation detectors and radio antennas. Prototype stations for this upgrade have been in operation for several years at both, the South Pole and the Auger Observatory, enabling cross-checks and potentially a cross-calibration of the energy scales between the two experiments. In this contribution, we present an analysis of air showers observed with the radio antennas of the IceCube-Gen2 prototype station, coinciding with detections by the water-Cherenkov detectors of the densest part of the Pierre Auger Observatory's surface array, featuring a 433 m spacing.

¹Full author list at <https://icecube.wisc.edu/collaboration/authors/>.

²Full author list at https://www.auger.org/archive/authors_icrc_2025.html.

*Speaker

1. Introduction

The IceCube Neutrino Observatory [1], located at the South Pole, includes a surface array (IceTop), consisting of ice-Cherenkov detectors which enable air-shower detection in the PeV to EeV range. The planned extension of the observatory, IceCube-Gen2 [2], is also designed to include a surface array [3]. The design consists of scintillator detectors rather than Cherenkov detectors for the detection of shower particles. The scintillators will be complemented by antennas for the detection of radio emission produced by the air shower. A prototype detector station comprising eight scintillators and three antennas has been running for several years at the South Pole [4, 5], and two more stations have been deployed in the 2024/2025 Pole season [6].

In addition, a prototype station was deployed at the Pierre Auger Observatory [7] in Argentina. The Pierre Auger Observatory is the world's largest cosmic-ray detector, consisting of a surface detector array (SD) of 1660 stations with a spacing of 1500 m overlooked by fluorescence telescopes. The SD also includes two areas of denser instrumentation with 750 m and 433 m spacing. The water-Cherenkov detectors of the SD have recently been upgraded with the addition of a scintillator detector and radio antenna each, as part of the AugerPrime upgrade [8]. The IceCube-Gen2 prototype station is located within the SD-433 area (Fig. 1). It provides an R&D location that is more accessible than the South Pole and allows exploration of possible synergies between the observatories.

The inclusion of radio antennas in these observatories allows for the detection of the radio emission produced by the charged particles in the shower as a result of the geomagnetic and Askaryan effects. They allow for an independent measurement of the shower energy as well as of the depth of shower maximum with the option of a 100% duty cycle, and are therefore valuable for calibration purposes, mass composition measurements, and tests of hadronic interaction models.

In this work, we describe the IceCube-Gen2 station deployed at the Pierre Auger Observatory, and demonstrate the successful observation of radio signals from air showers.

2. Prototype detector station

The layout of the detector station deployed at Auger closely follows the reference design of the IceCube-Gen2 station; in-situ pictures are shown in Fig. 2. It consists of a central pair of scintillator detectors from which three arms extend, with another pair of scintillator detectors at the end of each arm. In the middle of each arm, a radio antenna of the SKALAv2 design is located [9]. By

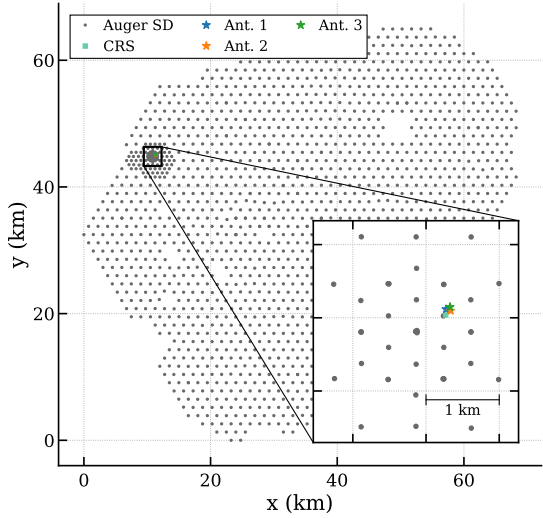


Figure 1: Positions of the SD stations of the Pierre Auger Observatory. The inset shows a zoom of the SD-433 area where the IceCube-Gen2 prototype station is located.



Figure 2: Left: Drone picture of the prototype station at the Pierre Auger Observatory. The container in the top left is the CRS (see text for details). Right: A pair of scintillator detectors (top) and a radio antenna (bottom) of the station.

the central scintillator pair, a box houses the data-acquisition (DAQ) system, known as TAXI. The station is located in the SD-433 area of the Observatory, near the *Central Radio Station* (CRS) of the *Auger Engineering Radio Array* (AERA) [10]. Power to the station is provided by solar panels and batteries located at the CRS, where also a WhiteRabbit switch is located, which enables communication and provides precision timing information for TAXI.

The nominal frequency band of the radio system is 70 MHz to 350 MHz. The radio signals are recorded by DRS4 chips on the TAXI. Data have been recorded with sampling rates of 1000 Msps and 800 Msps, always in 1024 bin waveforms. The readout of the radio data is triggered in two ways: a scintillator trigger, which is formed when six out of eight panels see a signal over threshold within 1 μ s, and a fixed-rate forced trigger. The former is used to look for air showers, while the latter is used to study the radio background. In this work, the scintillators are only used as a trigger for the radio readout; for more details about their design and operation, see Ref. [11].

3. Search for radio signals from air showers

To demonstrate the detection of radio signals from air showers, a simple analysis is performed, matching scintillator-triggered events with high-amplitude radio signals to events reconstructed by the Auger SD-433 array [12]. We use data recorded between January 2023 and February 2024. During this time, different modes of operation were tested. Importantly, the sampling rate for the radio data was changed from 1000 Msps to 800 Msps on October 20, 2023. The analysis is performed separately for the two periods, and results are compared for the obtained air-shower samples below. Other changes include the amount of time per day the collection of radio data is running (versus when only scintillator calibration data is collected), the SiPM bias voltage for the scintillators, and the individual scintillator trigger thresholds. This leads to the fractional runtime changing significantly throughout time, and to varying rates of the scintillator-triggered readout of the radio data, spanning a range between about 0.01 Hz and 0.12 Hz throughout the data period. However, in all cases, the energy threshold for the scintillator trigger is expected to be below the

energies at which radio emission becomes significant. The fixed-rate trigger, on the other hand, operated at a continuous 0.1 Hz throughout the data period.

In the following, we describe how the event search is performed, after which we discuss the final sample of air showers with identified radio signals.

3.1 Method

The identification of radio signals from air showers is performed in two main steps: 1. the selection of events triggered by the scintillator detectors of the station which also have a large amplitude signal in all three antennas and 2. looking for a corresponding event with a matching trigger time and directional reconstruction in the Auger SD-433 dataset.

The ambient radio spectrum as recorded by the antennas is shown in Fig. 3. The analysis is performed in the frequency band of 110 MHz to 185 MHz due to the large background at lower and higher frequencies, mainly from FM radio around 100 MHz and from a TV station around 200 MHz. The differences between the spectra recorded at 1000 Msps and 800 Msps likely reflect a time-dependence in the anthropogenic background.

Details of the analysis steps have been described before in Ref. [13]; we summarize them below. For details of the SD-433 event reconstruction, we refer to Refs. [14] and [12].

Selection of candidate radio events

- A basic processing is applied to the radio data, including corrections for artifacts in the waveforms, bandpass filtering to the 110 MHz to 185 MHz range, and the application of a frequency weighting scheme to further reduce the influence of narrow-band background [15].
- The forced-trigger data is used to obtain distributions of the signal-to-noise ratio (SNR) in radio background waveforms. The 95th percentile of the SNR values is calculated for the next step in the analysis. This is done for each polarization of each antenna separately.
- To select candidates for air-shower events with observed radio emission, the scintillator-triggered events are considered. All events which do not have at least one polarization per antenna with an SNR value higher than 95% of the background SNR values are rejected.
- For each passing event, a simple directional reconstruction is applied by fitting a plane shower front to the signal peak times in each antenna.

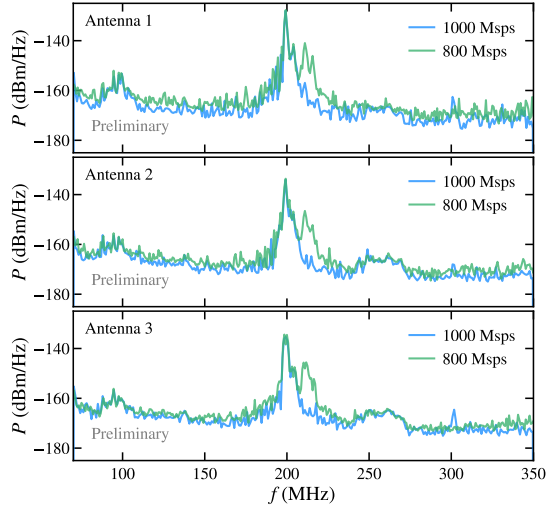


Figure 3: Frequency spectrum of the radio background recorded by the three antennas of the station at the Pierre Auger Observatory. In blue (green), the spectrum obtained in early (late) October 2023 with a sampling rate of 1000 Msps (800 Msps).

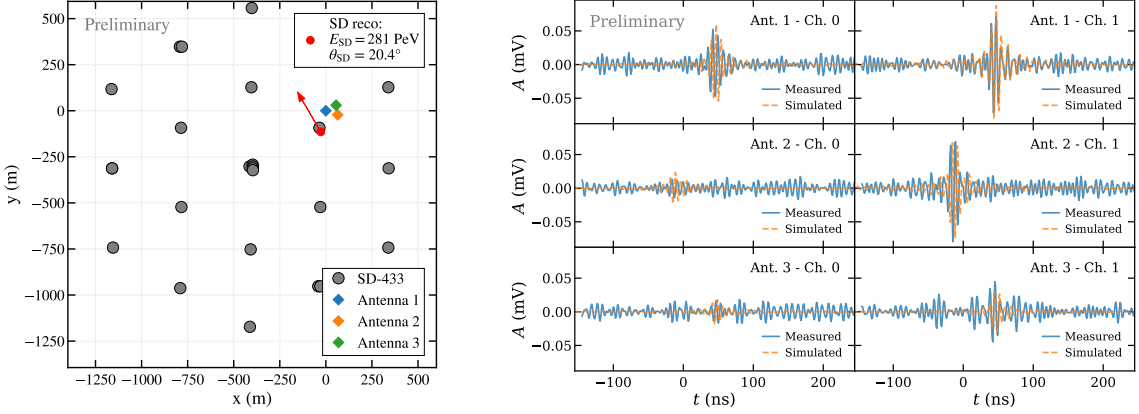


Figure 4: Example of an identified air-shower event. Left: The core position and direction from the SD-433 reconstructions compared to the antenna positions. Right: Comparison of the measured waveforms and waveforms from an air shower simulated based on the SD-433 reconstruction.

Matching with Auger SD-433 events

- The time offset between the IceCube-Gen2 prototype station and Auger SD is determined statistically by comparing a large number of scintillator-triggered events of the station to air-shower events recorded by SD. This is repeated every 12 hours due to a drift between the absolute times of the systems, which is taken into account in further analysis.
- For each radio event candidate, SD-433 events in a window of $\pm 50 \text{ ms}$ are considered after correcting for the time difference between the systems. (Due to the time drift between the systems and the imperfect corrections, this window is rather large. However, as the trigger rate of the SD-433 dataset is only around 0.01 Hz, chance coincidences are rare.)
- For each event found in the time window around the station trigger, the reconstructed directions from the radio signals and the SD-433 reconstruction are compared. To further ensure that the two events belong to the same air shower, the opening angle is required to be less than 5 degrees. (The event matching based on time and opening angle is visualized in Fig. 5, which is discussed more in the following section.)
- For each selected event, air-shower simulations are performed with CORSIKA [16], using the shower core position, direction, and energy from the SD-433 reconstruction as input parameters, assuming different primaries. The radio emission is simulated with CoREAS [17], and the response of the antennas and electronics chain is simulated. The simulated and measured waveforms are then compared for validation. A template matching is performed to find the best alignment between the two, after which a visual inspection is performed.

An example event identified following these steps is shown in Fig. 4. Note that deviations between the simulated and measured waveforms are expected due to uncertainties in the reconstructed core position, direction, and energy, in addition to the unknown depth of shower maximum.

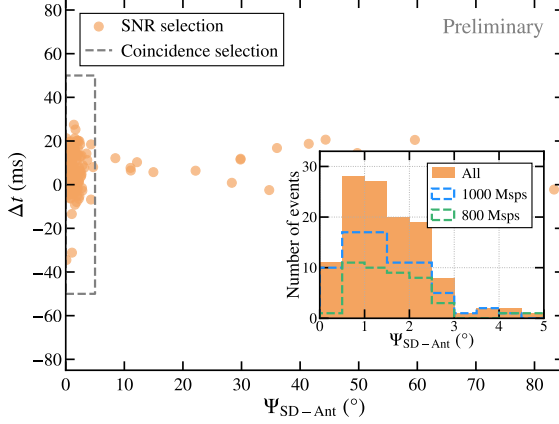


Figure 5: Time difference and opening angle between radio candidate events and SD-433 events. The box defines the selection of coincident events. The inset shows the opening angle distribution of selected events for the total sample, as well as the 1000 Msps and 800 Msps subsamples.

3.2 Identified air showers

We analyzed data recorded between January 1, 2023 and February 12, 2024. The radio data acquisition typically ran for 18 hours per day, with the other hours used to collect scintillator calibration data. Later in 2023, the radio data recording was increased to periods of 21-23 hours per day. Taking this into account, and removing periods of downtime due to hardware and software issues, a total runtime of 241.2 days was available for analysis. Following the method described above, a total of 135 events with radio emission matching an event reconstructed in SD-433 was found. Of these, 17 did not have a successful energy reconstruction from SD-433 and are excluded for the following discussion. After this, the average rate is 0.49 ± 0.05 events per day of runtime.

The sampling rate of the radio DAQ was changed from 1000 Msps to 800 Msps on October 20, 2023. The 1000 Msps data corresponds to a runtime of 143.3 days in which 74 events were found. The 800 Msps data corresponds to 97.9 days of runtime with 44 identified events. There is no significant difference in the event rates between the two periods.

The identification of the events based on the time and direction observed in both the prototype station and SD-433 is visualized in Fig. 5 for the full data period included in this analysis. SD-433 events with small time differences compared to the prototype station typically also cluster at small opening angles, indicating that these are real hybrid events. The opening angle distribution of the identified events, shown in the inset of the figure, peaks near 1° , indicating that even with three radio antennas, a good angular resolution is possible. Note that there is a tail of events at small time differences which have large opening angles; these are likely misreconstructed events which may be recoverable in future work.

The core positions for the identified events, as reconstructed by SD-433, are shown in Fig. 6 (left). All events cluster near the location of the antennas, mostly within a radius of ~ 250 m around the station center. In Fig. 6 (right), the reconstructed arrival directions are shown. We observe a tendency for events to appear more frequently at larger angles to the geomagnetic field direction, which is expected due to the radio emission produced by the geomagnetic effect. The area around the zenith is currently excluded from the event selection, as some DAQ artifacts not caught by our

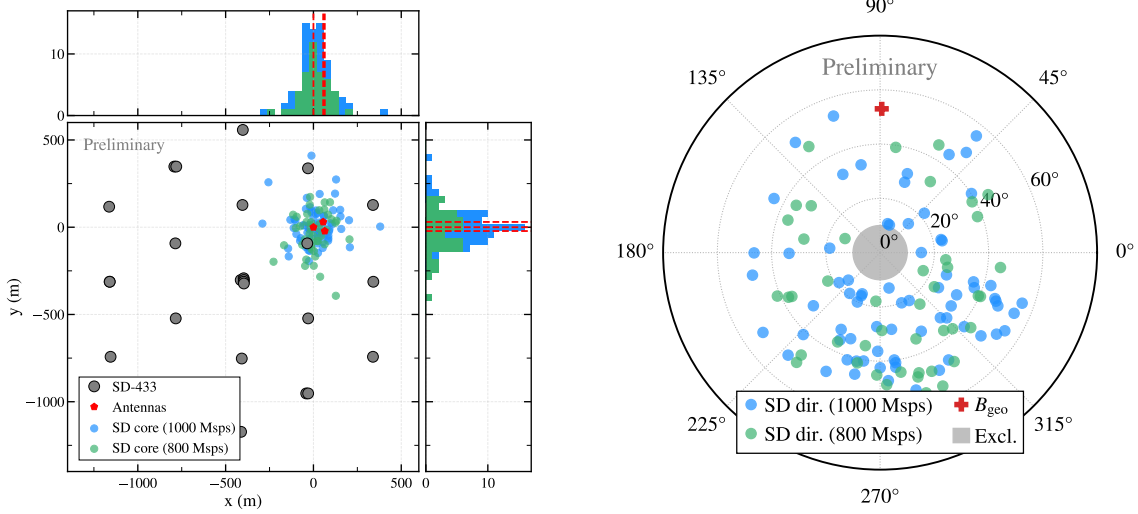


Figure 6: Shower geometry of the identified events as reconstructed with SD-433, for the 1000 Msps and 800 Msps subsamples. Left: Core positions compared to the position of the antennas. The dashed lines in the histograms represent the antenna positions. The coordinates have been centered on the position of Antenna 1. Right: Reconstructed arrival directions compared to the geomagnetic field direction. (The zenith is excluded due to occasional artifacts in the radio data.)

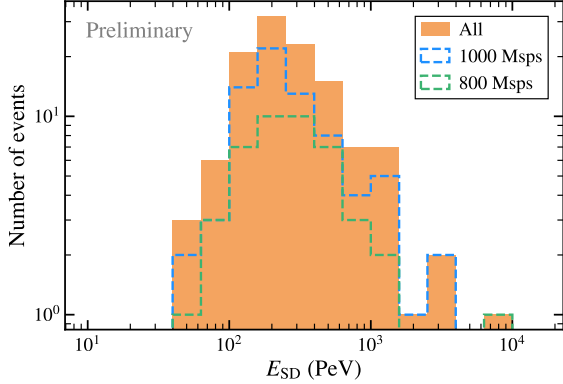


Figure 7: Distribution of the SD-433 reconstructed shower energies, for the total sample as well as the 1000 Msps and 800 Msps subsamples.

cleaning algorithms tend to mimic vertical air showers.

In Fig. 7, the distribution of energies reconstructed by SD-433 is shown. The lowest energy events are around several 10s of PeV and the distribution peaks around 200 PeV. SD-433 reaches full efficiency for showers below 40° around 63 PeV [12]. For the future, it would be of interest to study the efficiency for radio observation as a function of the SD-433 energy, given a certain shower geometry. A recently deployed array of 18 SKALA antennas is expected to reach full efficiency for the reconstruction based on radio signals around 300 PeV for showers with zenith angles below 30° [18].

4. Summary & Outlook

A prototype detector station for the surface component of the IceCube-Gen2 Observatory, consisting of scintillator panels and radio antennas, was deployed at the Pierre Auger Observatory and has been taking data for several years. First data from the station was used to successfully observe the radio emission from air showers trigger by the accompanying scintillators. By matching with showers reconstructed using the Auger SD-433 array, 118 events were identified in about 241 days of runtime, corresponding to a rate of 0.49 ± 0.05 events per day.

The selection of events with radio signals could be improved in the future, e.g. through more sophisticated SNR-based cuts, the use of neural networks for classifying and/or denoising [19], or by a more focused search for radio signals for events already reconstructed with SD-433. The successful radio detection of air showers with the station at this location suggests that future combined studies with the surface array of IceCube(-Gen2) and the Pierre Auger Observatory could be explored. Using the same antennas at both sites will reduce systematic uncertainties, e.g. in a comparison of the cosmic-ray energy scales in the overlapping energy range of the observatories [20].

References

- [1] **IceCube** Collaboration, M. G. Aartsen *et al.*, *JINST* **12** no. 03, (2017) P03012. [Erratum: *JINST* **19**, E05001 (2024)].
- [2] **IceCube-Gen2** Collaboration, M. G. Aartsen *et al.*, *J. Phys. G* **48** no. 6, (2021) 060501.
- [3] **IceCube-Gen2** Collaboration, F. G. Schroeder *et al.*, *PoS ICRC2021* (2021) 407.
- [4] **IceCube** Collaboration, R. Abbasi *et al.*, *PoS ICRC2021* (2021) 314.
- [5] **IceCube** Collaboration, A. Rehman *et al.*, *PoS ICRC2023* (2023) 291.
- [6] **IceCube** Collaboration, M. Venugopal, *PoS ICRC2025* (these proceedings) 427.
- [7] **Pierre Auger** Collaboration, A. Aab *et al.*, *Nucl. Instrum. Meth. A* **798** (2015) 172–213.
- [8] **Pierre Auger** Collaboration, A. Castellina, *EPJ Web Conf.* **210** (2019) 06002.
- [9] E. de Lera Acedo, N. Razavi-Ghods, N. Troop, N. Drought, and A. J. Faulkner, *Experimental Astronomy* **39** no. 3, (Oct., 2015) 567–594.
- [10] **Pierre Auger** Collaboration, P. Abreu *et al.*, *JINST* **7** (2012) P10011.
- [11] **IceCube** Collaboration, F. G. Schroeder *et al.*, *PoS ICRC2023* (2023) 342.
- [12] **Pierre Auger** Collaboration, G. Brichetto Orquera *et al.*, *PoS ICRC2023* (2023) 398.
- [13] **IceCube-Gen2** and **Pierre Auger** Collaborations, S. Verpoest *et al.*, *PoS ARENA2024* (2024) 037.
- [14] **Pierre Auger** Collaboration, P. Abreu *et al.*, *PoS ICRC2021* (2021) 224.
- [15] **IceCube** Collaboration, R. Abbasi *et al.*, *PoS ICRC2021* (2021) 317.
- [16] D. Heck *et al.*, *Forschungszentrum Karlsruhe Report FZKA-6019* (1998) .
- [17] T. Huege, M. Ludwig, and C. W. James, *AIP Conf. Proc.* **1535** no. 1, (2013) 128.
- [18] S. Verpoest, F. Schroeder, A. Novikov, A. Coleman, B. Flaggs, A. Weindl, M. Venugopal, C. Merx, and A. Haungs, *PoS UHECR2024* (2025) 122.
- [19] **IceCube** Collaboration, F. G. Schroeder and A. Rehman, *PoS ARENA2024* (2024) 034.
- [20] A. Coleman *et al.*, *Astropart. Phys.* **149** (2023) 102819.

- ⁶ Dept. of Physics, University of California, Berkeley, CA 94720, USA
⁷ Lawrence Berkeley National Laboratory, Berkeley, CA 94720, USA
⁸ Institut für Physik, Humboldt-Universität zu Berlin, D-12489 Berlin, Germany
⁹ Fakultät für Physik & Astronomie, Ruhr-Universität Bochum, D-44780 Bochum, Germany
¹⁰ Université Libre de Bruxelles, Science Faculty CP230, B-1050 Brussels, Belgium
¹¹ Vrije Universiteit Brussel (VUB), Dienst ELEM, B-1050 Brussels, Belgium
¹² Dept. of Physics, Simon Fraser University, Burnaby, BC V5A 1S6, Canada
¹³ Department of Physics and Laboratory for Particle Physics and Cosmology, Harvard University, Cambridge, MA 02138, USA
¹⁴ Dept. of Physics, Massachusetts Institute of Technology, Cambridge, MA 02139, USA
¹⁵ Dept. of Physics and The International Center for Hadron Astrophysics, Chiba University, Chiba 263-8522, Japan
¹⁶ Department of Physics, Loyola University Chicago, Chicago, IL 60660, USA
¹⁷ Dept. of Astronomy and Astrophysics, University of Chicago, Chicago, IL 60637, USA
¹⁸ Dept. of Physics, University of Chicago, Chicago, IL 60637, USA
¹⁹ Enrico Fermi Institute, University of Chicago, Chicago, IL 60637, USA
²⁰ Kavli Institute for Cosmological Physics, University of Chicago, Chicago, IL 60637, USA
²¹ Dept. of Physics and Astronomy, University of Canterbury, Private Bag 4800, Christchurch, New Zealand
²² Dept. of Physics, University of Maryland, College Park, MD 20742, USA
²³ Dept. of Astronomy, Ohio State University, Columbus, OH 43210, USA
²⁴ Dept. of Physics and Center for Cosmology and Astro-Particle Physics, Ohio State University, Columbus, OH 43210, USA
²⁵ Niels Bohr Institute, University of Copenhagen, DK-2100 Copenhagen, Denmark
²⁶ Dept. of Physics, TU Dortmund University, D-44221 Dortmund, Germany
²⁷ Dept. of Physics and Astronomy, Michigan State University, East Lansing, MI 48824, USA
²⁸ Dept. of Physics, University of Alberta, Edmonton, Alberta, T6G 2E1, Canada
²⁹ Erlangen Centre for Astroparticle Physics, Friedrich-Alexander-Universität Erlangen-Nürnberg, D-91058 Erlangen, Germany
³⁰ Physik-department, Technische Universität München, D-85748 Garching, Germany
³¹ Département de physique nucléaire et corpusculaire, Université de Genève, CH-1211 Genève, Switzerland
³² Dept. of Physics and Astronomy, University of Gent, B-9000 Gent, Belgium
³³ Dept. of Physics and Astronomy, University of California, Irvine, CA 92697, USA
³⁴ Karlsruhe Institute of Technology, Institute for Astroparticle Physics, D-76021 Karlsruhe, Germany
³⁵ Karlsruhe Institute of Technology, Institute of Experimental Particle Physics, D-76021 Karlsruhe, Germany
³⁶ Dept. of Physics, Engineering Physics, and Astronomy, Queen's University, Kingston, ON K7L 3N6, Canada
³⁷ Department of Physics & Astronomy, University of Nevada, Las Vegas, NV 89154, USA
³⁸ Nevada Center for Astrophysics, University of Nevada, Las Vegas, NV 89154, USA
³⁹ Dept. of Physics and Astronomy, University of Kansas, Lawrence, KS 66045, USA
⁴⁰ Dept. of Physics and Astronomy, University of Nebraska–Lincoln, Lincoln, Nebraska 68588, USA
⁴¹ Dept. of Physics, King's College London, London WC2R 2LS, United Kingdom
⁴² School of Physics and Astronomy, Queen Mary University of London, London E1 4NS, United Kingdom
⁴³ Centre for Cosmology, Particle Physics and Phenomenology - CP3, Université catholique de Louvain, Louvain-la-Neuve, Belgium
⁴⁴ Department of Physics, Mercer University, Macon, GA 31207-0001, USA
⁴⁵ Dept. of Astronomy, University of Wisconsin—Madison, Madison, WI 53706, USA
⁴⁶ Dept. of Physics and Wisconsin IceCube Particle Astrophysics Center, University of Wisconsin—Madison, Madison, WI 53706, USA
⁴⁷ Institute of Physics, University of Mainz, Staudinger Weg 7, D-55099 Mainz, Germany
⁴⁸ School of Physics and Astronomy, The University of Manchester, Oxford Road, Manchester, M13 9PL, United Kingdom
⁴⁹ Department of Physics, Marquette University, Milwaukee, WI 53201, USA
⁵⁰ Dept. of High Energy Physics, Tata Institute of Fundamental Research, Colaba, Mumbai 400 005, India
⁵¹ Institut für Kernphysik, Universität Münster, D-48149 Münster, Germany
⁵² Bartol Research Institute and Dept. of Physics and Astronomy, University of Delaware, Newark, DE 19716, USA
⁵³ Dept. of Physics, Yale University, New Haven, CT 06520, USA
⁵⁴ Columbia Astrophysics and Nevis Laboratories, Columbia University, New York, NY 10027, USA
⁵⁵ Dept. of Physics, University of Notre Dame du Lac, 225 Nieuwland Science Hall, Notre Dame, IN 46556-5670, USA
⁵⁶ Graduate School of Science and NITEP, Osaka Metropolitan University, Osaka 558-8585, Japan
⁵⁷ Dept. of Physics, University of Oxford, Parks Road, Oxford OX1 3PU, United Kingdom
⁵⁸ Dipartimento di Fisica e Astronomia Galileo Galilei, Università Degli Studi di Padova, I-35122 Padova PD, Italy
⁵⁹ Dept. of Physics, Drexel University, 3141 Chestnut Street, Philadelphia, PA 19104, USA
⁶⁰ Physics Department, South Dakota School of Mines and Technology, Rapid City, SD 57701, USA
⁶¹ Dept. of Physics, University of Wisconsin, River Falls, WI 54022, USA
⁶² Dept. of Physics and Astronomy, University of Rochester, Rochester, NY 14627, USA
⁶³ Department of Physics and Astronomy, University of Utah, Salt Lake City, UT 84112, USA
⁶⁴ Dept. of Physics, Chung-Ang University, Seoul 06974, Republic of Korea
⁶⁵ Oskar Klein Centre and Dept. of Physics, Stockholm University, SE-10691 Stockholm, Sweden

- ⁶⁶ Dept. of Physics and Astronomy, Stony Brook University, Stony Brook, NY 11794-3800, USA
⁶⁷ Dept. of Physics, Sungkyunkwan University, Suwon 16419, Republic of Korea
⁶⁸ Institute of Physics, Academia Sinica, Taipei, 11529, Taiwan
⁶⁹ Earthquake Research Institute, University of Tokyo, Bunkyo, Tokyo 113-0032, Japan
⁷⁰ Dept. of Physics and Astronomy, University of Alabama, Tuscaloosa, AL 35487, USA
⁷¹ Dept. of Astronomy and Astrophysics, Pennsylvania State University, University Park, PA 16802, USA
⁷² Dept. of Physics, Pennsylvania State University, University Park, PA 16802, USA
⁷³ Institute of Gravitation and the Cosmos, Center for Multi-Messenger Astrophysics, Pennsylvania State University, University Park, PA 16802, USA
⁷⁴ Dept. of Physics and Astronomy, Uppsala University, Box 516, SE-75120 Uppsala, Sweden
⁷⁵ Dept. of Physics, University of Wuppertal, D-42119 Wuppertal, Germany
⁷⁶ Deutsches Elektronen-Synchrotron DESY, Platanenallee 6, D-15738 Zeuthen, Germany
^a also at Institute of Physics, Sachivalaya Marg, Sainik School Post, Bhubaneswar 751005, India
^b also at Department of Space, Earth and Environment, Chalmers University of Technology, 412 96 Gothenburg, Sweden
^c also at INFN Padova, I-35131 Padova, Italy
^d also at Earthquake Research Institute, University of Tokyo, Bunkyo, Tokyo 113-0032, Japan
^e now at INFN Padova, I-35131 Padova, Italy

Acknowledgments

The authors gratefully acknowledge the support from the following agencies and institutions: USA – U.S. National Science Foundation-Office of Polar Programs, U.S. National Science Foundation-Physics Division, U.S. National Science Foundation-EPSCoR, U.S. National Science Foundation-Office of Advanced Cyberinfrastructure, Wisconsin Alumni Research Foundation, Center for High Throughput Computing (CHTC) at the University of Wisconsin–Madison, Open Science Grid (OSG), Partnership to Advance Throughput Computing (PATh), Advanced Cyberinfrastructure Coordination Ecosystem: Services & Support (ACCESS), Frontera and Ranch computing project at the Texas Advanced Computing Center, U.S. Department of Energy-National Energy Research Scientific Computing Center, Particle astrophysics research computing center at the University of Maryland, Institute for Cyber-Enabled Research at Michigan State University, Astroparticle physics computational facility at Marquette University, NVIDIA Corporation, and Google Cloud Platform; Belgium – Funds for Scientific Research (FRS-FNRS and FWO), FWO Odysseus and Big Science programmes, and Belgian Federal Science Policy Office (Belspo); Germany – Bundesministerium für Forschung, Technologie und Raumfahrt (BMFTR), Deutsche Forschungsgemeinschaft (DFG), Helmholtz Alliance for Astroparticle Physics (HAP), Initiative and Networking Fund of the Helmholtz Association, Deutsches Elektronen Synchrotron (DESY), and High Performance Computing cluster of the RWTH Aachen; Sweden – Swedish Research Council, Swedish Polar Research Secretariat, Swedish National Infrastructure for Computing (SNIC), and Knut and Alice Wallenberg Foundation; European Union – EGI Advanced Computing for research; Australia – Australian Research Council; Canada – Natural Sciences and Engineering Research Council of Canada, Calcul Québec, Compute Ontario, Canada Foundation for Innovation, WestGrid, and Digital Research Alliance of Canada; Denmark – Villum Fonden, Carlsberg Foundation, and European Commission; New Zealand – Marsden Fund; Japan – Japan Society for Promotion of Science (JSPS) and Institute for Global Prominent Research (IGPR) of Chiba University; Korea – National Research Foundation of Korea (NRF); Switzerland – Swiss National Science Foundation (SNSF).

- ¹⁰ Observatorio Pierre Auger, Malargüe, Argentina
¹¹ Observatorio Pierre Auger and Comisión Nacional de Energía Atómica, Malargüe, Argentina
¹² Universidad Tecnológica Nacional – Facultad Regional Buenos Aires, Buenos Aires, Argentina
¹³ University of Adelaide, Adelaide, S.A., Australia
¹⁴ Université Libre de Bruxelles (ULB), Brussels, Belgium
¹⁵ Vrije Universiteit Brussels, Brussels, Belgium
¹⁶ Centro Brasileiro de Pesquisas Fisicas, Rio de Janeiro, RJ, Brazil
¹⁷ Centro Federal de Educação Tecnológica Celso Suckow da Fonseca, Petropolis, Brazil
¹⁸ Instituto Federal de Educação, Ciência e Tecnologia do Rio de Janeiro (IFRJ), Brazil
¹⁹ Universidade de São Paulo, Escola de Engenharia de Lorena, Lorena, SP, Brazil
²⁰ Universidade de São Paulo, Instituto de Física de São Carlos, São Carlos, SP, Brazil
²¹ Universidade de São Paulo, Instituto de Física, São Paulo, SP, Brazil
²² Universidade Estadual de Campinas (UNICAMP), IFGW, Campinas, SP, Brazil
²³ Universidade Estadual de Feira de Santana, Feira de Santana, Brazil
²⁴ Universidade Federal de Campina Grande, Centro de Ciencias e Tecnologia, Campina Grande, Brazil
²⁵ Universidade Federal do ABC, Santo André, SP, Brazil
²⁶ Universidade Federal do Paraná, Setor Palotina, Palotina, Brazil
²⁷ Universidade Federal do Rio de Janeiro, Instituto de Física, Rio de Janeiro, RJ, Brazil
²⁸ Universidad de Medellín, Medellín, Colombia
²⁹ Universidad Industrial de Santander, Bucaramanga, Colombia
³⁰ Charles University, Faculty of Mathematics and Physics, Institute of Particle and Nuclear Physics, Prague, Czech Republic
³¹ Institute of Physics of the Czech Academy of Sciences, Prague, Czech Republic
³² Palacky University, Olomouc, Czech Republic
³³ CNRS/IN2P3, IJCLab, Université Paris-Saclay, Orsay, France
³⁴ Laboratoire de Physique Nucléaire et de Hautes Energies (LPNHE), Sorbonne Université, Université de Paris, CNRS-IN2P3, Paris, France
³⁵ Univ. Grenoble Alpes, CNRS, Grenoble Institute of Engineering Univ. Grenoble Alpes, LPSC-IN2P3, 38000 Grenoble, France
³⁶ Université Paris-Saclay, CNRS/IN2P3, IJCLab, Orsay, France
³⁷ Bergische Universität Wuppertal, Department of Physics, Wuppertal, Germany
³⁸ Karlsruhe Institute of Technology (KIT), Institute for Experimental Particle Physics, Karlsruhe, Germany
³⁹ Karlsruhe Institute of Technology (KIT), Institut für Prozessdatenverarbeitung und Elektronik, Karlsruhe, Germany
⁴⁰ Karlsruhe Institute of Technology (KIT), Institute for Astroparticle Physics, Karlsruhe, Germany
⁴¹ RWTH Aachen University, III. Physikalischs Institut A, Aachen, Germany
⁴² Universität Hamburg, II. Institut für Theoretische Physik, Hamburg, Germany
⁴³ Universität Siegen, Department Physik – Experimentelle Teilchenphysik, Siegen, Germany
⁴⁴ Gran Sasso Science Institute, L'Aquila, Italy
⁴⁵ INFN Laboratori Nazionali del Gran Sasso, Assergi (L'Aquila), Italy
⁴⁶ INFN, Sezione di Catania, Catania, Italy
⁴⁷ INFN, Sezione di Lecce, Lecce, Italy
⁴⁸ INFN, Sezione di Milano, Milano, Italy
⁴⁹ INFN, Sezione di Napoli, Napoli, Italy
⁵⁰ INFN, Sezione di Roma “Tor Vergata”, Roma, Italy
⁵¹ INFN, Sezione di Torino, Torino, Italy
⁵² Istituto di Astrofisica Spaziale e Fisica Cosmica di Palermo (INAF), Palermo, Italy
⁵³ Osservatorio Astrofisico di Torino (INAF), Torino, Italy
⁵⁴ Politecnico di Milano, Dipartimento di Scienze e Tecnologie Aerospaziali , Milano, Italy
⁵⁵ Università del Salento, Dipartimento di Matematica e Fisica “E. De Giorgi”, Lecce, Italy
⁵⁶ Università dell’Aquila, Dipartimento di Scienze Fisiche e Chimiche, L’Aquila, Italy
⁵⁷ Università di Catania, Dipartimento di Fisica e Astronomia “Ettore Majorana“, Catania, Italy
⁵⁸ Università di Milano, Dipartimento di Fisica, Milano, Italy
⁵⁹ Università di Napoli “Federico II”, Dipartimento di Fisica “Ettore Pancini”, Napoli, Italy
⁶⁰ Università di Palermo, Dipartimento di Fisica e Chimica ”E. Segre”, Palermo, Italy
⁶¹ Università di Roma “Tor Vergata”, Dipartimento di Fisica, Roma, Italy
⁶² Università Torino, Dipartimento di Fisica, Torino, Italy
⁶³ Benemérita Universidad Autónoma de Puebla, Puebla, México
⁶⁴ Unidad Profesional Interdisciplinaria en Ingeniería y Tecnologías Avanzadas del Instituto Politécnico Nacional (UPIITA-IPN), México, D.F., México
⁶⁵ Universidad Autónoma de Chiapas, Tuxtla Gutiérrez, Chiapas, México
⁶⁶ Universidad Michoacana de San Nicolás de Hidalgo, Morelia, Michoacán, México
⁶⁷ Universidad Nacional Autónoma de México, México, D.F., México
⁶⁸ Institute of Nuclear Physics PAN, Krakow, Poland

- ⁶⁹ University of Łódź, Faculty of High-Energy Astrophysics, Łódź, Poland
⁷⁰ Laboratório de Instrumentação e Física Experimental de Partículas – LIP and Instituto Superior Técnico – IST, Universidade de Lisboa – UL, Lisboa, Portugal
⁷¹ “Horia Hulubei” National Institute for Physics and Nuclear Engineering, Bucharest-Magurele, Romania
⁷² Institute of Space Science, Bucharest-Magurele, Romania
⁷³ Center for Astrophysics and Cosmology (CAC), University of Nova Gorica, Nova Gorica, Slovenia
⁷⁴ Experimental Particle Physics Department, J. Stefan Institute, Ljubljana, Slovenia
⁷⁵ Universidad de Granada and C.A.F.P.E., Granada, Spain
⁷⁶ Instituto Galego de Física de Altas Enerxías (IGFAE), Universidade de Santiago de Compostela, Santiago de Compostela, Spain
⁷⁷ IMAPP, Radboud University Nijmegen, Nijmegen, The Netherlands
⁷⁸ Nationaal Instituut voor Kernfysica en Hoge Energie Fysica (NIKHEF), Science Park, Amsterdam, The Netherlands
⁷⁹ Stichting Astronomisch Onderzoek in Nederland (ASTRON), Dwingeloo, The Netherlands
⁸⁰ Universiteit van Amsterdam, Faculty of Science, Amsterdam, The Netherlands
⁸¹ Case Western Reserve University, Cleveland, OH, USA
⁸² Colorado School of Mines, Golden, CO, USA
⁸³ Department of Physics and Astronomy, Lehman College, City University of New York, Bronx, NY, USA
⁸⁴ Michigan Technological University, Houghton, MI, USA
⁸⁵ New York University, New York, NY, USA
⁸⁶ University of Chicago, Enrico Fermi Institute, Chicago, IL, USA
⁸⁷ University of Delaware, Department of Physics and Astronomy, Bartol Research Institute, Newark, DE, USA

^a Max-Planck-Institut für Radioastronomie, Bonn, Germany

^b also at Kapteyn Institute, University of Groningen, Groningen, The Netherlands

^c School of Physics and Astronomy, University of Leeds, Leeds, United Kingdom

^d Fermi National Accelerator Laboratory, Fermilab, Batavia, IL, USA

^e Pennsylvania State University, University Park, PA, USA

^f Colorado State University, Fort Collins, CO, USA

^g Louisiana State University, Baton Rouge, LA, USA

^h now at Graduate School of Science, Osaka Metropolitan University, Osaka, Japan

ⁱ Institut universitaire de France (IUF), France

^j now at Technische Universität Dortmund and Ruhr-Universität Bochum, Dortmund and Bochum, Germany

Acknowledgments

The successful installation, commissioning, and operation of the Pierre Auger Observatory would not have been possible without the strong commitment and effort from the technical and administrative staff in Malargüe. We are very grateful to the following agencies and organizations for financial support:

Argentina – Comisión Nacional de Energía Atómica; Agencia Nacional de Promoción Científica y Tecnológica (ANPCyT); Consejo Nacional de Investigaciones Científicas y Técnicas (CONICET); Gobierno de la Provincia de Mendoza; Municipalidad de Malargüe; NDM Holdings and Valle Las Leñas; in gratitude for their continuing cooperation over land access; Australia – the Australian Research Council; Belgium – Fonds de la Recherche Scientifique (FNRS); Research Foundation Flanders (FWO), Marie Curie Action of the European Union Grant No. 101107047; Brazil – Conselho Nacional de Desenvolvimento Científico e Tecnológico (CNPq); Financiadora de Estudos e Projetos (FINEP); Fundação de Amparo à Pesquisa do Estado de Rio de Janeiro (FAPERJ); São Paulo Research Foundation (FAPESP) Grants No. 2019/10151-2, No. 2010/07359-6 and No. 1999/05404-3; Ministério da Ciência, Tecnologia, Inovações e Comunicações (MCTIC); Czech Republic – GACR 24-13049S, CAS LQ100102401, MEYS LM2023032, CZ.02.1.01/0.0/0.0/16_013/0001402, CZ.02.1.01/0.0/0.0/18_046/0016010 and CZ.02.1.01/0.0/0.0/17_049/0008422 and CZ.02.01.01/00/22_008/0004632; France – Centre de Calcul IN2P3/CNRS; Centre National de la Recherche Scientifique (CNRS); Conseil Régional Ile-de-France; Département Physique Nucléaire et Corpusculaire (PNC-IN2P3/CNRS); Département Sciences de l’Univers (SDU-INSU/CNRS); Institut Lagrange de Paris (ILP) Grant No. LABEX ANR-10-LABX-63 within the Investissements d’Avenir Programme Grant No. ANR-11-IDEX-0004-02; Germany – Bundesministerium für Bildung und Forschung (BMBF); Deutsche Forschungsgemeinschaft (DFG); Finanzministerium Baden-Württemberg; Helmholtz Alliance for Astroparticle Physics (HAP); Helmholtz-Gemeinschaft Deutscher Forschungszentren (HGF); Ministerium für Kultur und Wissenschaft des Landes Nordrhein-Westfalen; Ministerium für Wissenschaft, Forschung und Kunst des Landes Baden-Württemberg; Italy – Istituto Nazionale di Fisica Nucleare (INFN); Istituto Nazionale di Astrofisica (INAF); Ministero dell’Università e della Ricerca (MUR); CETEMPS Center of Excellence; Ministero degli Affari Esteri (MAE), ICSC Centro Nazionale di Ricerca in High Performance Computing, Big Data and Quantum Computing, funded by European Union NextGenerationEU, reference code CN_00000013; México – Consejo Nacional de Ciencia y Tecnología (CONACYT) No. 167733; Universidad Nacional Autónoma de México (UNAM); PAPIIT DGAPA-UNAM; The Netherlands – Ministry of Education, Culture and Science; Netherlands Organisation for Scientific Research (NWO); Dutch national e-infrastructure with the support of SURF Cooperative; Poland – Ministry of Education and Science, grants No. DIR/WK/2018/11 and 2022/WK/12; National Science Centre, grants No. 2016/22/M/ST9/00198, 2016/23/B/ST9/01635, 2020/39/B/ST9/01398, and 2022/45/B/ST9/02163; Portugal – Portuguese national funds and FEDER funds

within Programa Operacional Factores de Competitividade through Fundação para a Ciência e a Tecnologia (COMPETE); Romania – Ministry of Research, Innovation and Digitization, CNCS-UEFISCDI, contract no. 30N/2023 under Romanian National Core Program LAPLAS VII, grant no. PN 23 21 01 02 and project number PN-III-P1-1.1-TE-2021-0924/TE57/2022, within PNCDI III; Slovenia – Slovenian Research Agency, grants P1-0031, P1-0385, I0-0033, N1-0111; Spain – Ministerio de Ciencia e Innovación/Agencia Estatal de Investigación (PID2019-105544GB-I00, PID2022-140510NB-I00 and RYC2019-027017-I), Xunta de Galicia (CIGUS Network of Research Centers, Consolidación 2021 GRC GI-2033, ED431C-2021/22 and ED431F-2022/15), Junta de Andalucía (SOMM17/6104/UGR and P18-FR-4314), and the European Union (Marie Skłodowska-Curie 101065027 and ERDF); USA – Department of Energy, Contracts No. DE-AC02-07CH11359, No. DE-FR02-04ER41300, No. DE-FG02-99ER41107 and No. DE-SC0011689; National Science Foundation, Grant No. 0450696, and NSF-2013199; The Grainger Foundation; Marie Curie-IRSES/EPLANET; European Particle Physics Latin American Network; and UNESCO.